

Article

Synthesis of π -Conjugated Polymers Containing Benzotriazole Units via Palladium-Catalyzed Direct C-H Cross-Coupling Polycondensation for OLEDs Applications

Dong Han ¹, Jingwen Li ¹, Qiang Zhang ^{1,2,*}, Zewang He ¹, Zhiwei Wu ¹, Jingting Chu ¹ and Yan Lu ^{1,2,3,*} 

¹ School of Materials Science & Engineering, Tianjin University of Technology, Tianjin 300384, China; hl912928@163.com (D.H.); yixialjw@126.com (J.L.); JEFFHZW1995@163.com (Z.H.); wuzhiwei2021@163.com (Z.W.); chu945699645@126.com (J.C.)

² Tianjin Key Laboratory for Photoelectric Materials and Devices, Tianjin University of Technology, Tianjin 300384, China

³ Key Laboratory of Display Materials & Photoelectric Devices, Ministry of Education, Tianjin University of Technology, Tianjin 300384, China

* Correspondence: zhangqiang@email.tjut.edu.cn (Q.Z.); luyan@tjut.edu.cn (Y.L.)

Abstract: Four D- π -A conjugated polymers, namely P1–P4, which contain benzotriazole building blocks in their backbone as acceptor, are synthesized via palladium-catalyzed direct C-H cross-coupling polycondensation of 5,6-difluorobenzotriazole with different thiophene derivatives, including 3-octylthiophene, 2,2'-bithiophene, thieno[3,4-b][1,4]dioxine, and 4,4'-dioctyl-4H-silolo-[3,2-b:4,5-b']dithiophene as donor units, respectively. Taking the polymer P1 as an example, the chemical structure of the polymer is demonstrated by ¹H and ¹⁹F NMR spectra. The optical, electrochemical, and thermal properties of these polymers are assessed by UV-vis absorption and fluorescence spectroscopy, cyclic voltammetry (CV), and thermal gravimetric analysis (TGA), respectively. DFT simulations of all polymers are also performed to understand their physicochemical properties. Furthermore, P1 and P2, which have relatively higher molecular weights and better fluorescent quantum efficiency than those of P3 and P4, are utilized as lighting emitters for organic light-emitting diodes (OLEDs), affording promising green and red luminescence with 0.07% and 0.14% of maximum external quantum efficiency, respectively, based on a device with an architecture of ITO/PEDOT:PSS/PTAA/the polymer emitting layer/TPBi/LiF/Al.

Keywords: C-H cross-coupling; D- π -A conjugated polymer; benzotriazole; OLEDs



Citation: Han, D.; Li, J.; Zhang, Q.; He, Z.; Wu, Z.; Chu, J.; Lu, Y. Synthesis of π -Conjugated Polymers Containing Benzotriazole Units via Palladium-Catalyzed Direct C-H Cross-Coupling Polycondensation for OLEDs Applications. *Polymers* **2021**, *13*, 254. <https://doi.org/10.3390/polym13020254>

Received: 17 December 2020

Accepted: 10 January 2021

Published: 14 January 2021

Publisher's Note: MDPI stays neutral with regard to jurisdictional claims in published maps and institutional affiliations.



Copyright: © 2021 by the authors. Licensee MDPI, Basel, Switzerland. This article is an open access article distributed under the terms and conditions of the Creative Commons Attribution (CC BY) license (<https://creativecommons.org/licenses/by/4.0/>).

1. Introduction

Organic light-emitting diodes (OLEDs) have received much attention both in academia and industry owing to their wide applications in fullcolor displays and solid-state lighting. π -Conjugated polymers have many unique photophysical properties that are inherited from the delocalized electronic structures of their backbones and, thus, they exhibit promising advantages, such as solution-processing, light-weight, low-cost, and facile preparation of flexible devices in various functional applications, such as OLEDs, solar cells, field-effect transistors (FETs), photodetectors, etc. [1–6].

A variety of π -conjugated polymers have been synthesized based on reliable coupling methods including Suzuki–Miyaura [7], Stille [8], and Kumada–Corriu couplings [9], etc. For example, Todd and coworkers used brominated 5,6-difluorobenzotriazole and 4-hexylthiophene as starting materials and *i*PrMgCl·LiCl as Grignard reagents to synthesize the alternating polymer poly(5,6-difluorobenzotriazole-alt-4-hexylthiophene) via Kumada catalyst-transfer polycondensation [10]. In 2014, several benzotriazole-containing π -conjugated polymers were also achieved through Stille coupling reaction of 4,7-dibromo-5,6-difluorobenzotriazole with 2,5-bis(trimethylstannyl)thiophene derivatives for polymer field-effect transistors (FETs) applications [11]. These synthetic methods above for benzotriazole-based π -conjugated polymers generally require halogenations and/or organometallic pre-

functionalization steps of the corresponding monomers prior to polymerization. It is often difficult to synthesize and purify the metalated monomers due to their instability. In addition, in some cases, these polymerization processes can produce a toxic byproduct, for example, trialkyltin bromide. To circumvent these problems, direct arylation polymerization (DAP) has been developed, exhibiting several advantages, including fewer synthetic steps, easier purification of monomers, and reduced environmental pollution. For instance, Luscombe et al. successfully synthesized the alternating copolymer of 5,6-difluorobenzotriazole and 2,5-dithienylsilole with $M_n = 10,000$ via DAP [12]. Most recently, transition-metal catalyzed direct C-H coupling strategy was proposed and has been applied for preparing various π -conjugated polymers, including our work [13–17]. This synthetic protocol fully avoids the steps of pre-functionalized starting monomers, and allows straightforward access to π -conjugated polymers [13–28]. However, this method is mainly limited to the homo-coupling of some aromatic monomers such as thienopyrroledione (TPD) [13], bithiazole [14], benzodimidazole [25–27], and ester-functionalized thiophene [16–19] at present. Obviously, it is more challenging to achieve the highly selective cross-coupling of two different aromatic monomers as there are many possible multiple coupling patterns.

In this work, a series of D- π -A type conjugated polymers containing benzotriazole as acceptor units were successfully synthesized via Pd-catalyzed direct C-H cross-coupling polycondensation reaction of 5,6-difluorobenzotriazole with thiophene derivatives. Furthermore, the as-prepared polymers' physicochemical properties and light-emitting performance were also assessed.

2. Experimental

2.1. Materials

5,6-Difluoro-2-(2-hexyldecyl)-2H-benzo[*d*][1,2,3]triazole, 3-octylthiophene, 2,2'-bithiophene, thieno[3,4-*b*][1,4]dioxine, 4,4-dioctyl-4H-silolo[3,2-*b*:4,5-*b'*]dithiophene, palladium acetate ($\text{Pd}(\text{OAc})_2$), pivalic acid (PivOH), potassium carbonate (K_2CO_3), and silver carbonate (Ag_2CO_3) were purchased from Zhengzhou HQ Material Co., Ltd. (Zhengzhou, China) for direct use. *N,N*-Dimethylacetamide (DMAc) and xylene were obtained from J&K Chemical (Beijing, China) and used without further purification. Poly(sodium-p-styrenesulfonate) (PSS), poly(2,3-dihydrothieno-1,4-dioxin) (PEDOT), poly[bis(4-phenyl)(2,4,6-trimethylphenyl)amine] (PTAA), and 1,3,5-tris(1-phenyl-1H-benzimidazol-2-yl) benzene (TPBi) were provided by Xi'an Polymer Light Technology Co. (Xi'an, China).

2.2. Instruments

^1H and ^{13}C NMR spectra of polymers were measured on a Bruker AV400 at 25 °C utilizing the residual solvent peak as reference. Molecular weights of polymers were determined by gel permeation chromatography (GPC) on Waters 1525 equipped with Waters Styragel HT gel columns using tetrahydrofuran (THF) as eluent at 35 °C and monodisperse polystyrene as standard. Thermogravimetric analyses (TGA) were carried out on a Frontier Mid-IR FTIR/STA6000-TL9000-Clarus SQ8 instrument with a 10 °C·min⁻¹ heating rate under a purified nitrogen gas flow. Optical properties of polymers including UV-vis absorption and photoluminescence (PL) spectra were obtained on a Shimadzu UV-2550 and Hitachi F-4600, respectively. Solid-state samples for the test of photophysical property were prepared by spin-casting of polymers chloroform solutions on quartz plates. Optical bandgaps were calculated based on the onset of the absorption spectra of the thin film. Cyclic voltammetry (CV) measurements are carried out on a LK98B II electrochemical analyzer at room temperature with the scan rate was 100 mV s⁻¹. In this experiment, a conventional three-electrode configuration was adopted, i.e., a glassy carbon electrode as the working electrode, a saturated calomel electrode (SCE) as the reference electrode, and a Pt wire as the counter electrode. Acetonitrile, freshly prepared (CH_3CN) by distilling from calcium hydride (CaH) under dry N_2 , was used as solvent. Tetrabutylammonium phosphorus hexafluoride (Bu_4NPF_6) with a concentration of 0.1 M in CH_3CN was applied as the support electrolyte.

2.3. Synthesis of Polymer

The polymers were prepared according to a similar procedure as reported in our recent work [27]. In detail, 5,6-difluoro-2-(2-hexyldecyl)-2H-benzo[d][1,2,3]triazole (**1**) (113.7 mg, 0.3 mmol), 3-octylthiophene (58.8 mg, 0.3 mmol) were dissolved in 3 mL of DMAc/xylene (*v/v*, 10/1). Silver carbonate (248.2 mg, 0.9 mmol) and potassium carbonate (124.4 mg, 0.9 mmol), pivalic acid (61.3 mg, 0.6 mmol), Pd(OAc)₂ (6.7 mg, 10 mol%) were added into the above solution. The mixture was stirred for 48 h at 110 °C under N₂. After the mixture was cooled to room temperature, it was poured into cold methanol (100 mL). The precipitate was collected and subsequently subjected to successive Soxhlet extractions with anhydrous methanol and hexanes for 24 h to remove possible catalytic residues and oligomers. The residue was then extracted with chloroform for another 12 h. The CHCl₃ solution was concentrated to about 2 mL using a rotary evaporator and was then poured into methanol (60 mL). The precipitate was collected and dried under vacuum at 30 °C for 12 h to provide **P1** as a black solid (159 mg, 93 % yield). $M_n = 22.3$ kDa, PDI = 1.82 (GPC). ¹H NMR (400 MHz, CDCl₃) δ 8.38 (m, *J* = 10.5 Hz, 1H), 4.86–4.37 (m, 2H), 2.70 (s, 2H), 2.28 (s, 1H), 1.68 (s, 2H), 1.45–1.04 (m, 34H), 0.84 (s, 9H).

P2, **P3**, and **P4** were synthesized based on a similar procedure as that for **P1**, except for the use of different monomers. **P2**: 131 mg, 82% yield, $M_n = 28.1$ kDa, PDI = 1.22 (GPC). ¹H NMR (400 MHz, CDCl₃) δ 8.21 (m, 1H), 6.98 (br, 3H), 4.71 (d, 2H), 2.25 (s, 1H), 1.32 (d, 32H), 0.86 (s, 8H). **P3**: 15.6 mg, 10% yield, $M_n = 15.0$ kDa, PDI = 1.59 (GPC). ¹H NMR (400 MHz, CDCl₃) δ 4.75–3.96 (m, 6H), 2.25 (s, 1H), 1.41 (d, 24H), 0.87 (d, *J* = 7.2 Hz, 6H). **P4**: 47.8 mg, 20% yield, $M_n = 3.5$ kDa, PDI = 1.34 (GPC). ¹H NMR (400 MHz, CDCl₃) δ 6.98 (br, *J* = 15.4 Hz, 2H), 4.60 (d, 2H), 2.25 (s, 1H), 1.73–0.97 (m, 52H), 0.86 (s, 12H).

2.4. Device Fabrication and Characterization

The OLED devices with **P1** and **P2** as a light-emitting layer were fabricated with the following configuration: ITO/PSS:PEDOT/PTAA/polymer light-emitting layer/TPBi/LiF/Al.

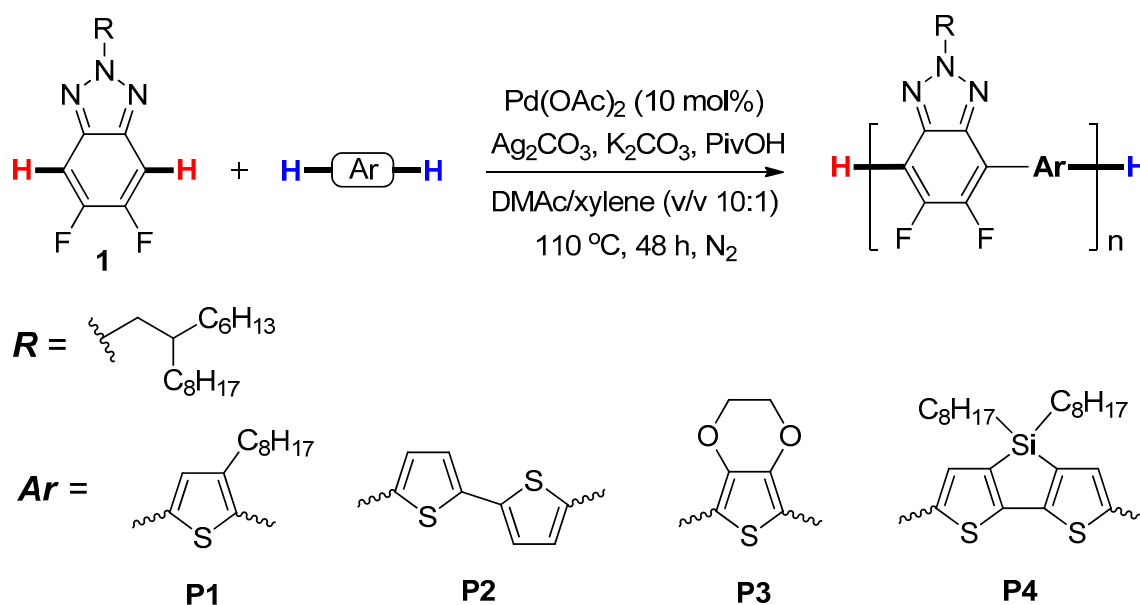
In this experiment, indium tin oxide (ITO) glass with a conductivity of 10 Ω /square was first pre-cleaned with acetone and ethanol under ultrasound and was subsequently treated in an ultraviolet–ozone chamber. A thin 40 nm-thick PSS-PEDOT layer was spin-coated onto the treated ITO glass which was placed on a hot plate at 3000 rpm for 10 min at 110 °C. The coated ITO glass was then transferred to a glovebox filled with N₂ and re-dried for 10 min at 110 °C. The solution of PTAA (5 mg) in 1 mL of DMF was then spin-coated onto the top of PSS:PEDOT layer on ITO to form an electron blocking layer with a thickness of 30 nm. After the above substrate was baked for 20 min at 100 °C, the toluene solution of **P1** or **P2** (10 mg/mL) was spin-coated onto PTAA layer to form a uniform 40 nm-thick light-emitting layer, which was followed by an annealing treatment for 10 min at 90 °C. Finally, using conventional thermal evaporation under vacuum, TPBi, LiF, and Al were deposited onto the surface of the active layer in sequence with the thicknesses of 30, 1, and 120 nm, respectively. The devices provided an active area of 5 \times 3 mm². Based on the above devices, the electroluminescence (EL) spectra, current density–voltage (*J*–*V*) and luminance–voltage (*L*–*V*) were obtained on a Keithley 2400 Source Meter system. The luminance of OLEDs was measured with a PhotoResearch SpectraScan PR-650 Colorimeter.

3. Results and Discussion

3.1. Synthesis and Characterization of Polymers

As depicted in Scheme 1, **P1**–**P4** were prepared by Pd-catalyzed direct C–H cross-coupling reaction of 5,6-difluoro-2-(2-hexyldecyl)-2H-benzotriazole (**1**) with four different thiophene derivatives, including 3-octylthiophene, 2,2'-bithiophene, thieno[3,4-*b*][1,4] dioxine, and 4,4'-dioctyl-4H-silolo-[3,2-*b*:4,5-*b'*]dithiophene under the optimized conditions as reported in our recent work [29], namely, Pd(OAc)₂ (10 mol%) as catalyst, Ag₂CO₃ (3.0 equiv) as oxidant, K₂CO₃ (3.0 equiv) as base, PivOH (2.0 equiv) as additive, and DMAc/xylene (*v/v*, 10/1) as solvents at 110 °C for 48 h. A branched side chain (2-hexyldecyl) was attached to benzotriazole units, aiming to improve the solubility of com-

bound **1** and the resultant copolymers in the common organic solvents, such as DMAc, DMF, CHCl_3 , etc. [11]. The results of the polycondensation reactions and the thermophysical properties of **P1–P4** were shown in Table 1.



Scheme 1. Synthetic routes of the polymers **P1–P4**.

Table 1. Results of the polycondensation and the thermostability of **P1–P4**.

Entry	Polymer ^a	M_n^b	M_w^b	M_w/M_n^b	Yield/% ^c	T_d^d
1	P1	22,300	40,580	1.82	93	317
2	P2	28,100	34,280	1.22	82	385
3	P3	15,000	23,850	1.59	10	256
4	P4	3500	4690	1.34	20	392

^a Reaction conditions: benzotriazole monomer (1.0 equiv), thiophene monomer (1.0 equiv), Pd(OAc)_2 (10 mol%), Ag_2CO_3 (3.0 equiv), K_2CO_3 (3.0 equiv), and PivOH (2.0 equiv) in DMAc/xylene (v/v, 10/1) for 48 h at 110 °C under N_2 ; ^b Estimated by GPC measurements (eluent: THF; standard: polystyrene); ^c Isolated yield after purification.

^d The 5% weight-loss temperature under N_2 atmosphere.

The polycondensation of 5,6-difluoro-2-(2-hexyldecyl)-2H-benzotriazole (**1**) with 3-octylthiophene provides the polymer **P1** with an average molecular weight of $M_n = 22,300$ in an excellent yield (93%). In the case of 2,2'-bithiophene as donor units, **P2** with the highest molecular weight of $M_n = 28,100$ was obtained in a good yield (82%). By contrast, the polymerization reaction of **1** with thieno[3,4-*b*][1,4]dioxine mainly yielded an insoluble solid in common organic solvents, and only a small number of products can be isolated by Soxhlet extractions with CHCl_3 to provide a total yield of about 10%. This result may be due to the cross-linking reaction in multiple C-H systems [30,31]. Dithienosilole cores are common building blocks of various active materials used in photovoltaics, FETs, and OLEDs, etc. [32–36] because of their strong donating electron ability, photostability, and chemical stability. Under the same reaction conditions as that for **P1–P3**, the polycondensation of **1** with 4,4'-diocetyl-4H-silolo-[3,2-*b*:4,5-*b'*]dithiophene yields a soluble polymer **P4** in CHCl_3 with low yield (about 20%) (Table 1, entry 4), which is similar to the case of **P3**. Most of the as-prepared polymers exhibit good thermal stability with the degradation temperatures at 5% weight loss are 385, 317, and 392 °C for **P1**, **P2**, and **P4**, respectively (Table 1), which is suitable for the applications in the semiconductor devices.

3.2. Structural Characterization

The chemical structure of polymers was determined by ^1H and ^{19}F NMR spectra (Figure 1 and Figures S1–S8). Taking **P1** as an example, all characteristic proton peaks corre-

sponding to the benzotriazole and thiophene units can be observed as shown in Figure 1A, which is similar to the analogous polymers obtained via the Kumada method except for different alkyl side chains as reported by Bielawski and co-workers [10]. As seen in Figure 1A, the multiple peaks at 4.60–4.76 ppm (a in Figure 1A) and the broad peak at 2.28 ppm (b in Figure 1A) were assigned to the $-\underline{C}H_2$ groups close to the triazole ring and $-\underline{C}H$ signal of the branched groups, respectively. The peak at 2.70 nm (c in Figure 1A) corresponds to $-\underline{C}H_2$ groups of thiophene side chains. It was noted that the signal of aromatic hydrogen of thiophene units (d in Figure 1A) significantly shifted to low field compared with the corresponding thiophene monomer, which was possibly caused by $F \cdots H$ noncovalent interaction between the fluorine atoms on benzotriazole unit and the hydrogen atoms on thiophene units as demonstrated by our recent work [29] and the literature [11].

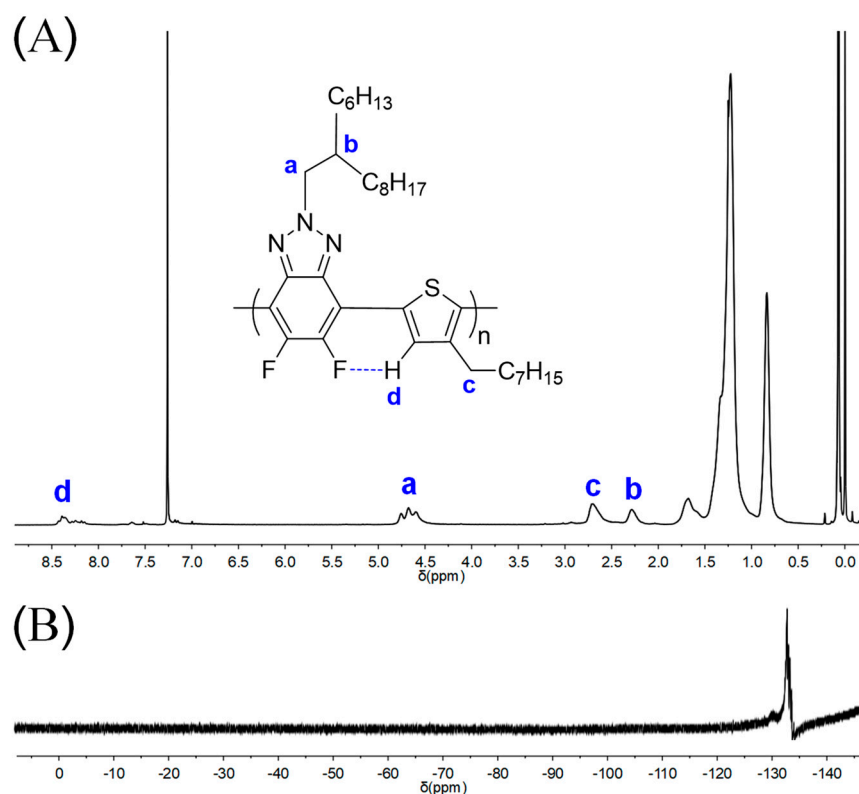


Figure 1. 1H NMR (A) and ^{19}F NMR (B) of **P1** in $CDCl_3$.

Besides, ^{19}F NMR was also applied to confirm the polymers' chemical structure since it has many merits, including high sensitivity, little interference, a large range of chemical shifts, and similar structures that are not easy to overlap, etc. As depicted in Figure 1B, the ^{19}F NMR of **P1** displayed an obvious main peak at -133.0 ppm that corresponds to the fluorine atoms on the polymeric chains. The remaining weak signals could be assigned to the end groups, where the fluorine atoms are not chemically equivalent to those along the backbone [37]. All the NMR results of **P1** suggest an alternating structure along the polymer main chain.

3.3. DFT Simulation

Density functional theory (DFT) simulation was performed at the B3LYP/6-31G* level using Gaussian 09 programs to check the effect of the structure of thiophene donor units on the polymer backbone on the HOMO and LUMO energy levels of the resultant polymers. In this study, four repeated D-A units were used and all side chains were replaced with methyl groups to simplify the calculation. The HOMO and LUMO level values were obtained by MO topologies on the basis of the optimized geometry. As shown in Figure 2, the contour plots indicated the effective separation of HOMO and LUMO levels for all polymers **P1–P4**,

which is beneficial to charge-carrier transport. Thus, these polymers were suitable for active materials of OLED devices. Additionally, it can be clearly seen from the molecular orbital diagrams that the HOMO energy levels of the four polymers all remain delocalized along the main chain of polymers, and the HOMO energy levels of **P1–P4** are -4.74 , -4.71 , -4.72 , and -4.47 eV, respectively. While the electron density is successively distributed on the whole D-A units, the LUMO values of **P1–P4** are calculated to be -2.61 , -2.64 , -1.98 , and -2.47 eV, respectively. It is important to note that the thiophene segments tend to be trans-coplanar with benzotriazole units in the optimized geometries of **P1** (Figure 2), where the sulfur atom of the thiophene unit is in the opposite position to the fluorine atom of the thiazole unit. This conformation is undoubtedly conducive to the formation of F \cdots H non-covalent interactions as demonstrated by ^1H NMR spectra shown in Figure 1A.

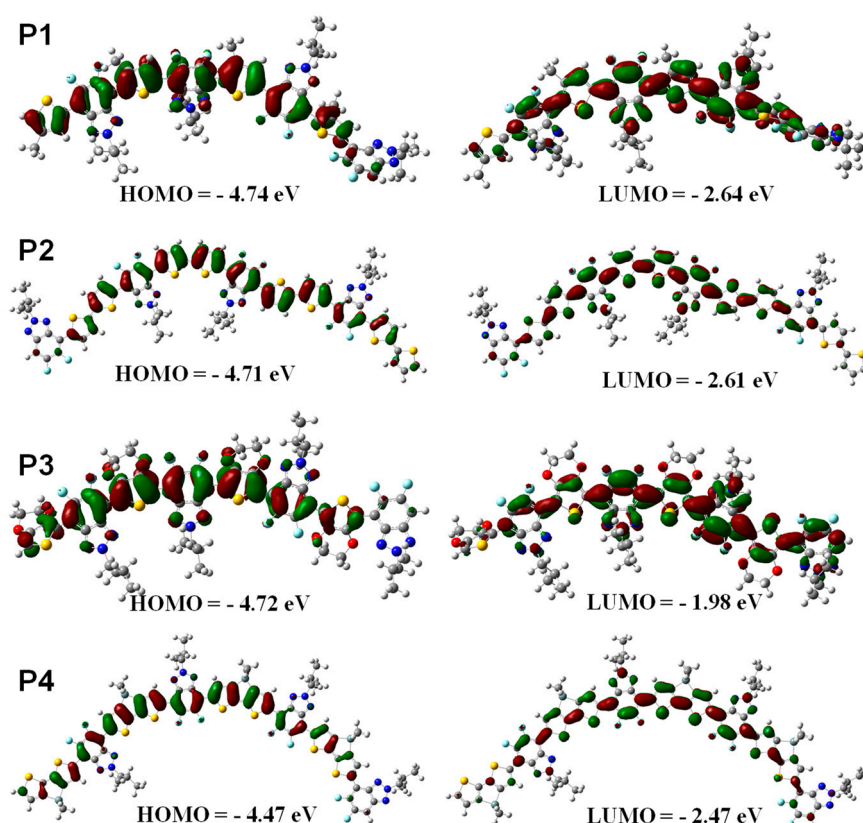


Figure 2. Optimized geometries and molecular orbital surfaces for the HOMO and LUMO values of **P1–P4** obtained using a DFT/B3LYP/6-31G* method.

3.4. UV–vis Absorption Spectra

The UV–vis absorption spectra of **P1–P4** in dilute chloroform (CHCl_3) solutions and in film states were measured on a Shimadzu UV-2550 spectrometer. The concentration of the polymer in CHCl_3 solution was 10^{-5} mol/L based on repeated units. The film samples were prepared by casting the chloroform solutions (3 mg/mL) on the surface of quartz and subsequently annealing for 10 min at 100°C . Their UV–vis absorption spectra of polymer solutions and thin films are presented in Figure 3, and the absorption maxima and the optical band gaps estimated from the absorption edge of the thin film are listed in Table 2.

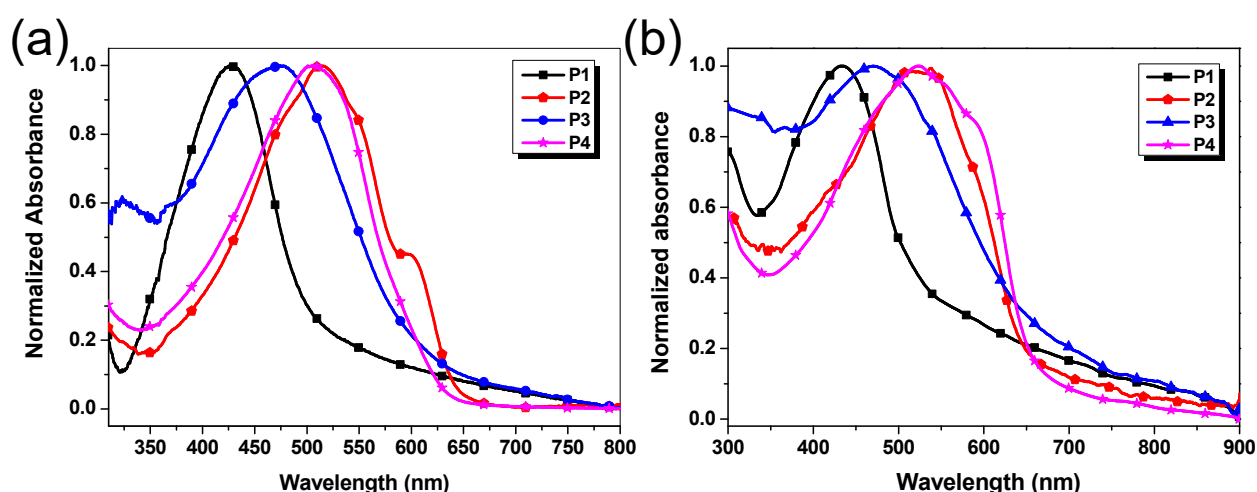


Figure 3. Normalized absorption spectra of **P1–P4** (a) in dilute chloroform solution (1×10^{-5} mol/L) and (b) in the thin film state (spin-cast from chloroform solution).

Table 2. Photophysical and electrochemical properties of **P1–P4**.

Entry	UV-vis			PL		CV		
	$\lambda_{\max}^{\text{Sol}}$ (nm)	$\lambda_{\max}^{\text{Film}}$ (nm)	E_g^{opt} (eV) ^a	$\lambda_{\max}^{\text{Sol}}$ (nm)	$\lambda_{\max}^{\text{Film}}$ (nm)	HOMO (eV) ^b	LUMO (eV) ^b	E_g^{cv} (eV) ^b
P1	427	428	2.16	542	560	−5.57	−3.60	1.97
P2	515, 596	510	1.81	575, 614	723	−5.69	−3.68	2.01
P3	471	468	1.85	564	-	−5.45	−3.59	1.86
P4	506	523	1.88	577, 616	-	−5.67	−3.58	2.09

^a Estimated from the absorption edge of the thin film. ^b Estimated from the cyclic voltammetry. $E_{\text{HOMO}} = -(4.8 + E_{\text{onset}}^{\text{ox}} - E_{\text{Fc}/\text{Fc}^+}^{\text{ox}})$ [eV]; $E_{\text{LUMO}} = -(4.8 + E_{\text{onset}}^{\text{red}} - E_{\text{Fc}/\text{Fc}^+}^{\text{red}})$ [eV]. $E_g^{\text{cv}} = E_{\text{HOMO}} - E_{\text{LUMO}}$.

As shown in Figure 3a and Table 2, the λ_{\max} of **P1–P4** in CHCl_3 solutions are 427, 515, 471, and 506 nm, respectively. Compared with **P1**, a remarkable redshift by 88 nm was observed for **P2** in CHCl_3 solutions, possibly due to **P2** having longer conjugated chains and a more efficient conjugated effect caused by smaller steric hindrance between benzotriazole units and dithiophene units. In addition, the λ_{\max} of all polymers in the thin film states exhibit negligible changes in comparison with that in solutions beside **P4**. The results should be attributed to only **P4** tending to form a more coplanar configuration between benzotriazole segments and silole ring in the solid-state due to the completely symmetrical and rigidly planar structure of silole units as demonstrated by DFT calculation (Figure 2). The optical band gaps (E_g^{opt}) of **P1–P4** were determined to be 2.16, 1.81, 1.85, and 1.88 eV, respectively, from the onsets of the spectra in the films. The results are close to the corresponding E_g^{opt} values of the other benzotriazole-based D- π -A conjugated polymers reported in the literature, including ours [9,27].

3.5. Photoluminescence Property

Figure 4a shows the photoluminescence (PL) spectra in CHCl_3 solutions. **P1–P4** exhibit broad emission peaks in the range of 480–770 nm upon excitation at 420 nm. In the case of **P2** and **P4**, the obvious shoulder bands at about 630 nm could be attributed to the intramolecular charge transfer (ICT) from thiophene units to benzotriazole units (Figure 4a) [38,39]. Additionally, it was noted that emission peaks of polymers vary with the different donor units, exhibiting a bathochromic displacement observed in the following order: **P1** < **P3** < **P2** \approx **P4** (Figure 4a). Thus, the polymers **P2** and **P4** with the more extended conjugated backbones show the maximum emission peaks at the highest wavelengths between 550 and 650 nm (Figure 4a).

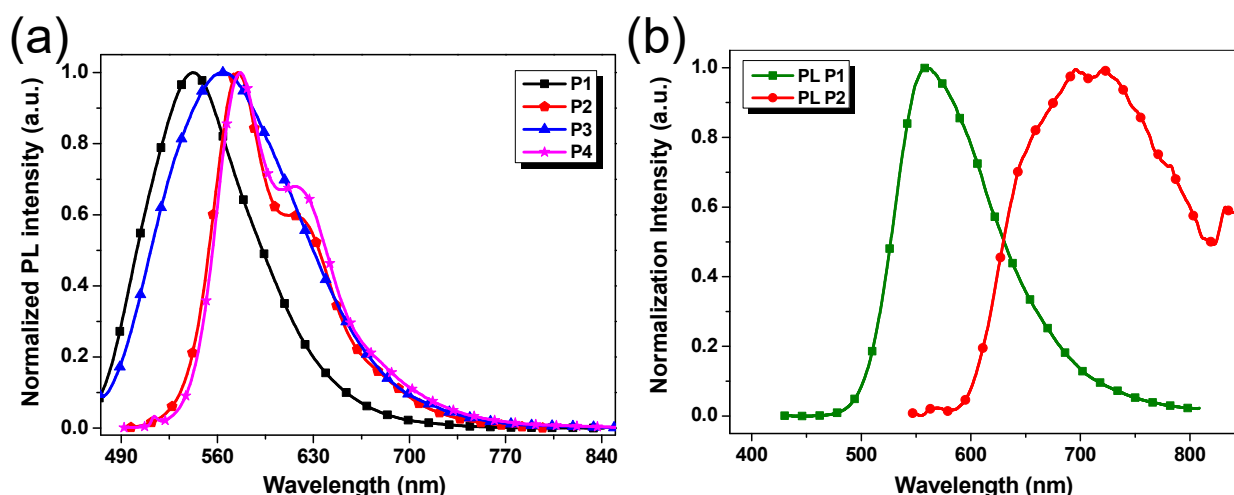


Figure 4. (a) Normalized PL spectra of **P1–P4** in dilute chloroform solutions (1×10^{-5} mol/L); (b) Normalized PL spectra in the thin film states of **P1** and **P2**.

Different emission behavior of the polymers was noticed in solid-state. **P1** maintained a similar emission profile to that in solution but consisted of a larger spectral domain, extended to most of the visible light region from 500 to 700 nm. The solid-state **P2** displayed a very wide emission extended into the near-infrared domain, with an emission peak located at near 700 nm (Figure 4b). Compared with the emission peak of **P2** in solution, its significant red-shift in thin-film state was noted. This should be attributed to more effective conjugation of polymer chains due to the intramolecular rotation that was restricted in solid-state. For the films of **P3** and **P4**, only very weak emissions were observed (not provided), which agrees with the results of similar polymers reported in the literature [40].

3.6. Electrochemical Property

The electrochemical properties of all polymers **P1–P4** were assessed by standard cyclic voltammetry (CV) using a saturated calomel electrode as reference electrode and the energy level of ferrocene/ferrocenium (-4.80 eV) as the internal standard (Figures S10 and S11). The energy levels of **P1–P4**, calculated on the basis of CV curves, are presented in Table 2. The HOMO levels of **P1–P4** are -5.57 , -5.69 , -5.45 , and -5.67 eV, respectively versus Fc/Fc^+ , and obviously lower than that of classical poly(3-hexylthiophene) (P3HT) materials (-5.10 eV) [41]. The results also indicate that the HOMO levels of benzotriazole-based conjugated polymers can be finely tuned by the introduction of different donor units. After magnification of the CV plots, the onsets of reduction potentials ($E_{\text{onset}}^{\text{red}}$) could be determined to be -0.73 , -0.81 , -0.82 , and -0.83 V for **P1–P4**, respectively. Hence, the LUMO energy levels of polymers **P1–P4** can be obtained to be -3.60 , -3.68 , -3.59 , and -3.58 eV, respectively, versus Fc/Fc^+ according to the corresponding $E_{\text{onset}}^{\text{red}}$. Since the conjugated polymers containing fluorinated benzotriazole segments can display excellent oxidative stability due to the stabilized HOMO and LUMO levels by the strong inductive effect of fluorine atoms [11,42], such polymer materials should have a huge potential for application in various photoelectric devices.

3.7. Electroluminescence Characteristics

Considering that **P1** and **P2** have relatively high M_n and good fluorescent quantum efficiency in solutions ($\eta = 0.3837$ and 0.3805 for **P1** and **P2**, respectively, measured on a FLS1000 fluorescence spectrometer, Edinburgh, UK), the solution-processed OLED devices with the **P1** and **P2** as emissive layers were fabricated based on the following configuration: ITO/PEDOT:PSS/PTAA/emissive layer/TPBi/LiF/Al. Figure 5 shows the electroluminescent (EL) spectra of the devices with the **P1** and **P2** as the emissive layer, respectively. The emission maxima of **P1** and **P2**-based EL devices were 544 and 640 nm, respectively, which

were slightly blue-shifted in comparison with the corresponding photoluminescence ones in the solid films as shown in Figure 4b. These results suggest that the color tuning on the EL device of benzotriazole-based polymers through the incorporation of various donor units on their backbone is feasible.

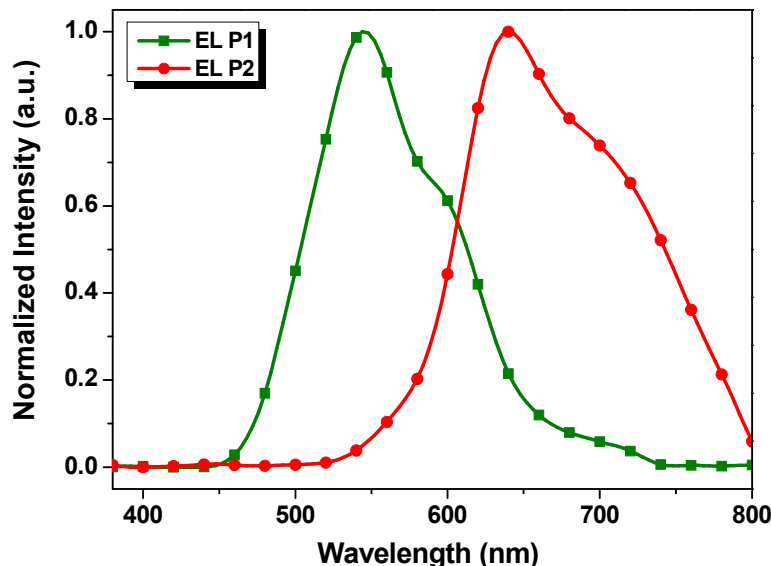


Figure 5. EL spectra P1 and P2-based devices.

Figure 6 shows the typical EL performances of P1 and P2-based devices and their EL characteristics that were also listed in Table 3. The rectification behavior of P1 and P2-based devices can be observed from their J - V curves (Figure S12) originating from the intrinsic properties of the diodes. The turn-on voltages (V_{on}) of P1- and P2-based devices were 4.0 and 3.0 V, respectively, as shown in Figure 6a. The P2-based device provided a higher luminance and current efficiency than that of P1 at a certain bias, as shown in Figure 6a,b. As a result, the maximum power efficiency ($\eta_p = 0.13$ lm/W) and the maximum external quantum efficiency ($EQE_{max} = 0.14\%$) for P2-based OLED devices, which is almost twice as much as that for P1-based devices (Figure 6c,d). The P1-based device exhibited a bright green emission with CIE coordinates of (0.40, 0.52) (Figure 6e), while a red emission with CIE coordinates of (0.66, 0.33) at 1200 cd/m² was observed for P2-based devices (Figure 6f). This result indicates P2 is a promising red emissive material for OLEDs.

Table 3. Luminescence characteristics of P1 and P2-based OLED devices.

Polymer	λ_{max}^{EL} (nm)	V_{on} (V)	Luminance (cd/m ²)	η_c (cd/A)	η_p (lm/W)	EQE_{max} (%)	CIE (x, y)
P1	544	4.0	774	0.12	0.059	0.07	(0.40, 0.52)
P2	640	3.0	1178	0.25	0.13	0.14	(0.66, 0.33)

V_{on} , voltage required for 1 cd/m²; η_c , maximum current efficiency; η_p , maximum power efficiency; EQE_{max} , maximum external quantum efficiency; CIE, chromaticity coordinate.

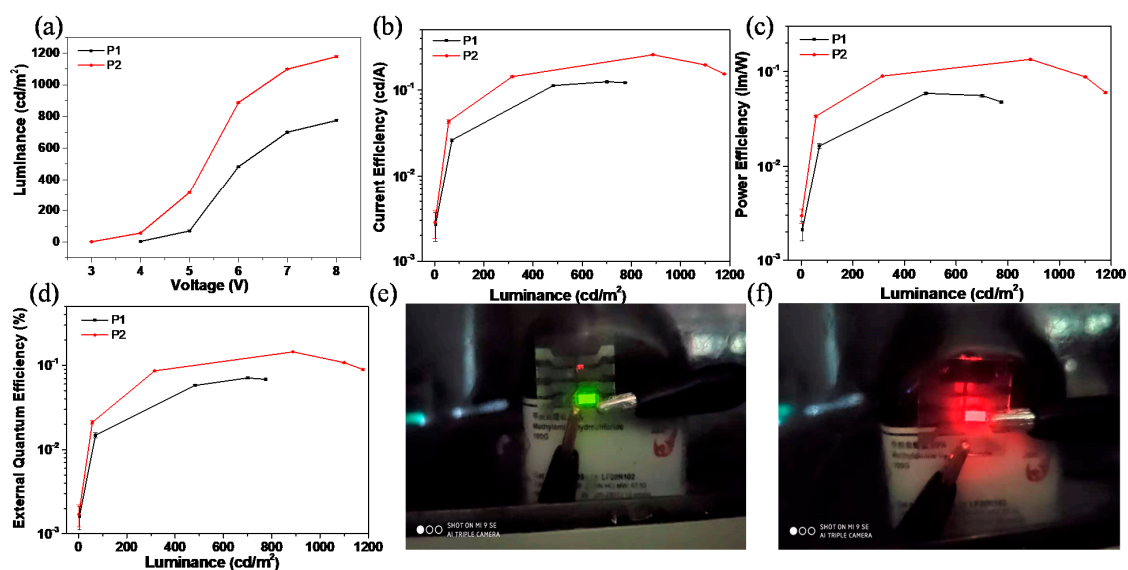


Figure 6. (a) The luminance–voltage (L – V) characteristics; (b) Current efficiency–luminance (J – L) curves; (c) Power efficiency *versus* luminance plots; (d) External quantum efficiency–luminance characteristics of P1 and P2. (e) The photograph of P1-based device with green emission at 8 V; (f) The photograph of P2-based device with red emission at 8 V.

4. Conclusions

Four benzotriazole-based π -conjugated polymers with donor-acceptor alternating structure were successfully prepared via Pd-catalyzed direct C–H cross-coupling polycondensation. The protocol offers a straightforward and effective assessment of such polymers without any pre-functionalized steps. This work extends the range of aromatic monomers for direct C–H cross-coupling polycondensation and achieves the effective copolymerization of electron-deficient benzotriazole with electron-rich thiophene derivatives in a structurally controllable mode. Although the as-synthesized polymer materials only displayed moderate OLED performances, the present method could have enormous potential for the synthesis of various semiconducting materials by tuning donor and acceptor units for different organic optoelectronic device applications.

Supplementary Materials: The supplementary materials are available online at <https://www.mdpi.com/2073-4360/13/2/254/s1>. Figures S1–S8: ¹H NMR and ¹⁹F NMR Spectra of P1–P4; Figure S9: TGA curves of P1–P4; Figure S10: Cyclic voltammograms of P1–P4; Figure S11: Schematic energy-level diagrams of P1–P4; Figure S12: The current density–voltage curve of P1 and P2-based devices.

Author Contributions: Investigation, D.H., J.L., Q.Z., Z.H., Z.W. and J.C.; Project administration, Q.Z. and Y.L.; Supervision, Y.L.; Validation, D.H., J.L. and Q.Z.; Writing—original draft, D.H. and Q.Z.; Writing—review & editing, Y.L. All authors have read and agreed to the published version of the manuscript.

Funding: The authors are grateful for the financial assistance of the NSFC (No. 21604063), the Natural Science Foundation of Tianjin (No. 18JCZDJC34600), the Program for Prominent Young College Teachers and Youth Reserve Talent of Tianjin Educational Committee, the Scientific Development Foundation of Tianjin Education Commission (2017ZD14) and Undergraduate Innovation and Entrepreneurship Training Program (201910060093) for financial support.

Institutional Review Board Statement: Not applicable.

Informed Consent Statement: Not applicable.

Data Availability Statement: The data presented in this study are available on request from the corresponding author.

Conflicts of Interest: The authors declare no conflict of interest.

References

1. Hildner, R.; Köhler, A.; Müller-Buschbaum, P.; Panzer, F.; Thelakkat, M. π -Conjugated Donor Polymers: Structure Formation and Morphology in Solution, Bulk and Photovoltaic Blends. *Adv. Energy Mater.* **2017**, *7*, 1700314. [[CrossRef](#)]
2. Wang, C.; Dong, H.; Hu, W.; Liu, Y.; Zhu, D. Semiconducting π -Conjugated Systems in Field-Effect Transistors: A Material Odyssey of Organic Electronics. *Chem. Rev.* **2012**, *112*, 2208–2267. [[CrossRef](#)] [[PubMed](#)]
3. Zuo, G.; Abdalla, H.; Kemerink, M. Conjugated Polymer Blends for Organic Thermoelectrics. *Adv. Electron. Mater.* **2019**, *5*, 1800821. [[CrossRef](#)]
4. Heeger, A.J. Semiconducting Polymers: The Third Generation. *Chem. Soc. Rev.* **2010**, *39*, 2354–2371. [[CrossRef](#)] [[PubMed](#)]
5. Popov, A.; Brasiunas, B.; Damaskaite, A.; Plikusiene, I.; Ramanavicius, A.; Ramanaviciene, A. Electrodeposited Gold Nanostructures for the Enhancement of Electrochromic Properties of PANI-PEDOT Film Deposited on Transparent Electrode. *Polymers* **2020**, *12*, 2778. [[CrossRef](#)]
6. Popov, A.; Brasiunas, B.; Mikoliunaite, L.; Bagdziunas, G.; Ramanavicius, A.; Ramanaviciene, A. Comparative Study of Polyaniline (PANI), Poly(3,4-ethylenedioxythiophene) (PEDOT) and PANI-PEDOT Films Electrochemically Deposited on Transparent Indium Thin Oxide Based Electrodes. *Polymer* **2019**, *172*, 133–141. [[CrossRef](#)]
7. Sakamoto, J.; Rehahn, M.; Wegner, G.; Schlüter, A.D. Suzuki Polycondensation: Polyarylenes à la Carte. *Macromol. Rapid Commun.* **2009**, *30*, 653–687. [[CrossRef](#)]
8. Carsten, B.; He, F.; Son, H.J.; Xu, T.; Yu, L. Stille Polycondensation for Synthesis of Functional Materials. *Chem. Rev.* **2011**, *111*, 1493–1528. [[CrossRef](#)]
9. Yokozawa, T.; Yokoyama, A. Chain-Growth Condensation Polymerization for the Synthesis of Well-Defined Condensation Polymers and π -Conjugated Polymers. *Chem. Rev.* **2009**, *109*, 5595–5619. [[CrossRef](#)]
10. Todd, A.D.; Bielawski, C.W. Controlled Synthesis of an Alternating Donor-Acceptor Conjugated Polymer via Kumada Catalyst-Transfer Polycondensation. *ACS Macro Lett.* **2015**, *4*, 1254–1258. [[CrossRef](#)]
11. Yum, S.; An, T.K.; Wang, X.; Lee, W.; Uddin, M.A.; Kim, Y.J.; Nguyen, T.L.; Xu, S.; Hwang, S.; Park, C.E.; et al. Benzotriazole-Containing Planar Conjugated Polymers with Noncovalent Conformational Locks for Thermally Stable and Efficient Polymer Field-Effect Transistors. *Chem. Mater.* **2014**, *26*, 2147–2154. [[CrossRef](#)]
12. Scott, C.N.; Bisen, M.D.; Stemer, D.M.; McKinnon, S.; Luscombe, C.K. Direct Arylation Polycondensation of 2,5-Dithienylsilole with a Series of Difluorobenzodiimine-Based Electron Acceptors. *Macromolecules* **2017**, *50*, 4623–4628. [[CrossRef](#)]
13. Zhang, Q.; Wan, X.; Lu, Y.; Li, Y.; Li, Y.; Li, C.; Wu, H.; Chen, Y. The Synthesis of 5-Alkyl[3,4-c]thienopyrrole-4,6-dione-Based Polymers Using a Pd-catalyzed Oxidative C-H/C-H Homopolymerization Reaction. *Chem. Commun.* **2014**, *50*, 12497–12499. [[CrossRef](#)] [[PubMed](#)]
14. Zhang, Q.; Li, Y.; Lu, Y.; Zhang, H.; Li, M.; Yang, Y.; Wang, J.; Chen, Y.; Li, C. Pd-catalysed Oxidative C-H/C-H Coupling Polymerization for Polythiazole-Based Derivatives. *Polymer* **2015**, *68*, 227–233. [[CrossRef](#)]
15. Zhang, Q.; Chang, M.; Lu, Y.; Sun, Y.; Li, C.; Yang, X.; Zhang, M.; Chen, Y. A Direct C-H Coupling Method for Preparing π -Conjugated Functional Polymers with High Regioregularity. *Macromolecules* **2018**, *51*, 379–388. [[CrossRef](#)]
16. Zhang, Q.; Li, Y.; Deng, L.; Zhao, L.; Li, C.; Lu, Y. Synthesis of Highly Regioregular, Head-to-Tail Coupled Poly(3-octylesterthiophene) via C-H/C-H Coupling Polycondensation. *Chin. J. Polym. Sci.* **2018**, *36*, 1019–1026. [[CrossRef](#)]
17. Deng, L.; Zhang, Q.; Zhao, L.; Lu, Y. Direct C-H Coupling Polymerization of Asymmetric Monomer: Synthesis and Properties of Regioregular Ppoly(alkyl thiophene-3-carboxylates). *Eur. Polym. J.* **2018**, *109*, 72–81. [[CrossRef](#)]
18. Gobalasingham, N.S.; Noh, S.; Thompson, B.C. Palladium-Catalyzed Oxidative Direct Arylation Polymerization (Oxi-DARp) of an Ester-Functionalized Thiophene. *Polym. Chem.* **2016**, *7*, 1623–1631. [[CrossRef](#)]
19. Gobalasingham, N.S.; Pankow, R.M.; Thompson, B.C. Synthesis of Random Poly(hexyl thiophene-3-carboxylate) Copolymers via Oxidative Direct Arylation Polymerization (oxi-DARp). *Polym. Chem.* **2017**, *8*, 1963–1971. [[CrossRef](#)]
20. Gobalasingham, N.S.; Thompson, B.C. Direct Arylation Polymerization: A Guide to Optimal Conditions for Effective Conjugated Polymers. *Prog. Polym. Sci.* **2018**, *83*, 135–201. [[CrossRef](#)]
21. Yang, Y.; Lan, J.; You, J. Oxidative C-H/C-H Coupling Reactions between Two (Hetero)arenes. *Chem. Rev.* **2017**, *117*, 8787–8863. [[CrossRef](#)] [[PubMed](#)]
22. Kang, L.J.; Xing, L.; Luscombe, C.K. Exploration and Development of Gold- and Silver-Catalyzed Cross Dehydrogenative Coupling toward Donor-Acceptor π -Conjugated Polymer Synthesis. *Polym. Chem.* **2019**, *10*, 486–493. [[CrossRef](#)]
23. Collier, G.S.; Reynolds, J.R. Exploring the Utility of Buchwald Ligands for C–H Oxidative Direct Arylation Polymerizations. *ACS Macro Lett.* **2019**, *8*, 931–936. [[CrossRef](#)]
24. Aoki, H.; Saito, H.; Shimoyama, Y.; Kuwabara, J.; Yasuda, T.; Kanbara, T. Synthesis of Conjugated Polymers Containing Octafluorobiphenylene Unit via Pd-Catalyzed Cross-Dehydrogenative-Coupling Reaction. *ACS Macro Lett.* **2018**, *7*, 90–94. [[CrossRef](#)]
25. Guo, Q.; Wu, D.; You, J. Oxidative Direct Arylation Polymerization Using Oxygen as the Sole Oxidant: Facile, Green Access to Bithiazole-Based Polymers. *ChemSusChem* **2016**, *9*, 2765–2768. [[CrossRef](#)]
26. Guo, Q.; Jiang, R.; Wu, D.; You, J. Rapid Access to 2,2'-Bithiazole-Based Copolymers via Sequential Palladium-Catalyzed C-H/C-X and C-H/C-H Coupling Reactions. *Macromol. Rapid Commun.* **2016**, *37*, 794–798. [[CrossRef](#)]

27. Huang, Q.; Qin, X.; Li, B.; Lan, J.; Guo, Q.; You, J. Cu-catalysed Oxidative C-H/C-H Coupling Polymerisation of Benzodiazoles: An Efficient Approach to Regioregular Polybenzodiazoles for Blue-Emitting Materials. *Chem. Commun.* **2014**, *50*, 13739–13741. [[CrossRef](#)]
28. Yang, Y.; Nishiura, M.; Wang, H.; Hou, Z. Metal-Catalyzed C-H Activation for Polymer Synthesis and Functionalization. *Coord. Chem. Rev.* **2018**, *376*, 506–532. [[CrossRef](#)]
29. Li, J.; Han, D.; Zhang, Q.; HE, Z.; Lu, Y. Synthesis and Properties of Fluorinated Benzotriazole-Based Donor-Acceptor-Type Conjugated Polymers via Pd-Catalyzed Direct C-H/C-H Coupling Polymerization. *J. Polym. Sci.* **2021**. [[CrossRef](#)]
30. Pankow, R.M.; Ye, L.; Thompson, B.C. Influence of An Ester Directing-Group on Defect Formation in the Synthesis of Conjugated Polymers via Direct Arylation Polymerization (DAP) Using Sustainable Solvents. *Polym. Chem.* **2019**, *10*, 4561–4572. [[CrossRef](#)]
31. Lombeck, F.; Marx, F.; Strassel, K.; Kunz, S.; Lienert, C.; Komber, H.; Friend, R.; Sommer, M. To Branch or not to Branch: C-H Selectivity of Thiophene-Based Donor-Acceptor-Donor Monomers in Direct Arylation Polycondensation Exemplified by PCDTBT. *Polym. Chem.* **2017**, *8*, 4738–4745. [[CrossRef](#)]
32. Adachi, Y.; Ooyama, Y.; Ren, Y.; Yin, X.; Jäkle, F.; Ohshita, J. Hybrid Conjugated Polymers with Alternating Dithienosilole or Dithienogermole and Tricoordinate Boron Units. *Polym. Chem.* **2018**, *9*, 291–299. [[CrossRef](#)]
33. Fei, Z.; Kim, Y.; Smith, J.; Domingo, E.B.; Stingelin, N.; McLachlan, M.A.; Song, K.; Anthopoulos, T.D.; Heeney, M. Comparative Optoelectronic Study between Copolymers of Peripherally Alkylated Dithienosilole and Dithienogermole. *Macromolecules* **2012**, *45*, 735–742. [[CrossRef](#)]
34. Zhong, L.; Bin, H.; Angunawela, I.; Jia, Z.; Qiu, B.; Sun, C.; Li, X.; Zhang, Z.; Ade, H.; Li, Y. Effect of Replacing Thiophene by Selenophene on the Photovoltaic Performance of Wide Bandgap Copolymer Donors. *Macromolecules* **2019**, *52*, 4776–4784. [[CrossRef](#)]
35. Hu, H.; Ye, L.; Ghasemi, M.; Balar, N.; Rech, J.J.; Stuard, S.J.; You, W.; O'Connor, B.T.; Ade, H. Highly Efficient, Stable, and Ductile Ternary Nonfullerene Organic Solar Cells from a Two-Donor Polymer Blend. *Adv. Mater.* **2019**, *31*, 1808279. [[CrossRef](#)] [[PubMed](#)]
36. Tang, A.; Song, W.; Xiao, B.; Guo, J.; Min, J.; Ge, Z.; Zhang, J.; Wei, Z.; Zhou, E. Benzotriazole-Based Acceptor and Donors, Coupled with Chlorination, Achieve a High V_{oc} of 1.24 V and an Efficiency of 10.5% in Fullerene-Free Organic Solar Cells. *Chem. Mater.* **2019**, *31*, 3941–3947. [[CrossRef](#)]
37. Livi, F.; Gobalasingham, N.S.; Bundgaard, E.; Thompson, B.C. Influence of Functionality on Direct Arylation of Model Systems as a Route Toward Fluorinated Copolymers via Direct Arylation Polymerization (DAP). *J. Polym. Sci. Part A Polym. Chem.* **2015**, *53*, 2598–2605. [[CrossRef](#)]
38. Wu, W.-C.; Liu, C.-L.; Chen, W.-C. Synthesis and Characterization of New Fluorene-Acceptor Alternating and Random Copolymers for Light-Emitting Applications. *Polymer* **2006**, *47*, 527–538. [[CrossRef](#)]
39. Torres-Moya, I.; Vázquez-Guilló, R.; Fernández-Palacios, S.; Carrillo, J.R.; Díaz-Ortiz, Á.; López Navarrete, J.T.; Ponce Ortiz, R.; Ruiz Delgado, M.C.; Mallavia, R.; Prieto, P. Fluorene-Based Donor-Acceptor Copolymers Containing Functionalized Benzotriazole Units: Tunable Emission and their Electrical Properties. *Polymers* **2020**, *12*, 256. [[CrossRef](#)]
40. Tutuncu, E.; Cihaner, A.; Icli Ozkut, M. Synthesis and Electropolymerization of a Donor-Acceptor-Donor Trimeric Monomer Containing 3,4-Propylenedioxythiophene and Dithienosilole Units. *Eur. Polym. J.* **2019**, *118*, 239–243. [[CrossRef](#)]
41. Kim, J.-H.; Park, J.B.; Kim, H.U.; Kang, I.-N.; Hwang, D.-H. High Open-Circuit Voltage Organic Photovoltaic Cells Fabricated Using Semiconducting Copolymers Consisting of Bithiophene and Fluorinated Quinoxaline or Triazole Derivatives. *Synth. Met.* **2014**, *194*, 88–96. [[CrossRef](#)]
42. Chen, J.; Yan, Z.; Tang, L.; Uddin, M.A.; Yu, J.; Zhou, X.; Yang, K.; Tang, Y.; Shin, T.J.; Woo, H.Y.; et al. 1,4-Di(3-alkoxy-2-thienyl)-2,5-Difluorophenylene: A Building Block Enabling High-Performance Polymer Semiconductors with Increased Open-Circuit Voltages. *Macromolecules* **2018**, *51*, 5352–5363. [[CrossRef](#)]